Vol 18 No 6, June 2009
1674-1056/2009/18(06)/2529-06

Chinese Physics B

© 2009 Chin. Phys. Soc.
and IOP Publishing Ltd

Propagation properties of a modified surface plasmonic waveguide with an arc slot*

Xue Wen-Rui(薛文瑞)†, Guo Ya-Nan(郭亚楠), and Zhang Wen-Mei(张文梅)

College of Physics and Electronic Engineering, Shanxi University, Taiyuan 030006, *China*

(Received 31 October 2008; revised manuscript received 11 December 2008)

We introduce a modified surface plasmonic waveguide with an arc slot. The dependences of distribution of energy flux density, effective index, propagation length and mode area of the symmetric mode supported by this waveguide on geometrical parameters and working wavelength are analysed by using the finite-difference frequency-domain (FDFD) method. Results show that the energy flux density distributes mainly in four corners which are formed by two arcs, and the closer to the corners it is, the stronger the energy flux density will be. The effective index, the propagation length and the mode area are influenced by geometrical parameters, including the width, the thickness and the arc radius of the surface plasmonic waveguide, as well as the working wavelength. It has been shown that the surface plasmonic waveguide with an arc slot has better propagation properties than the surface plasmonic waveguide with a straight slot. This work may be helpful for applying the slot surface plasmonic waveguide to integrated photonics.

Keywords: surface plasmons, optical waveguides
PACC: 7320M, 4280L

1. Introduction

During the past few years, surface plasmon polariton (SPP)-based waveguides have been a subject of intensive research.[1−4] Such waveguides provide a new mechanism of guiding the propagation of light in the form of SPP along the surface of metals. Because the SPP has a lateral scale of subwavelength, it can be used to overcome the diffraction limit that exists in conventional or photonic crystal waveguides, and to fulfil the further miniaturization of photonic devices and the high integration density of photonic chips.

Using thin metal films as surface plasmonic waveguides (SPWs)[5] was first proposed, but their applications were restricted due to the lack of lateral confinement. Therefore, metal films with finite size,[6] a metal rod with a square cross section,[7] an improved metal strip with finite size and width,[8] and other one-dimensional metal optical waveguides[9,10] are proposed. At present, SPWs with various geometries that could confine light in two dimensions have been reported, such as gap SPWs,[11−13] slot SPWs,[14,15] wedge SPWs,[16] trench SPWs,[17−20] mixed SPWs,[21] heterostructured SPWs,[22−25] and nanoparticle SPWs.[26−28]

In the present paper, a modified surface plasmonic waveguide with an arc slot is designed and its propagation properties are investigated by using the finite-difference frequency-domain method. We mainly investigate the effective index, the propagation length, and the mode area influenced by geometrical parameters and working wavelengths of the waveguide.

2. Structure and simulation method

The cross section of SPW structure proposed in this paper is shown in Fig.1. The SPW is composed of a piece of thin metal film with the width $2b$ and height $2t$, and a circular part with radius r which is caved in the symmetrical centre of the thin metal film.

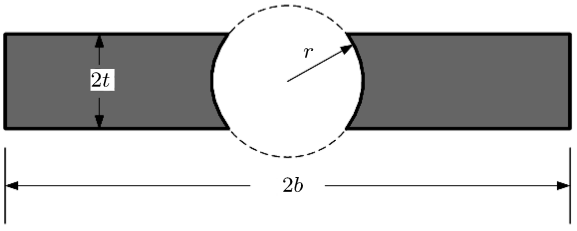


Fig.1. Cross section of the surface plasmonic waveguide with an arc slot.

*Project supported by the National Natural Science Foundation of China (Grant No 60771052) and the Natural Science Foundation of Shanxi Province, China (Grant No 2006011029).
†E-mail: wrxue@sxu.edu.cn

The main methods of investigating the propagation properties of a surface plasmonic waveguide are classified into two groups, one is the method in time domain and the other is the method in frequency domain. The former is used to perform the calculation in time domain, and the latter in frequency domain. Both methods allow us to directly use experimental data of the dielectric constant of noble metal. The 2D full-vectorial finite-difference frequency-domain (FDFD) method[29−31] is used to study the propagation properties of our proposed SPW structure. This is a simple and effective numerical simulation approach.

Supposing that the propagation constant in the z direction is β, each field component is expressed in the following form: $\phi(x, y, z) = \phi(x, y)\exp(j\beta z)$, where ϕ denotes an arbitrary field component. According to the theory of 2D FDFD, we can obtain two eigenvalue equations as follows:

$$\begin{bmatrix} Q_{xx} & Q_{xy} \\ Q_{yx} & Q_{yy} \end{bmatrix} \begin{bmatrix} H_x \\ H_y \end{bmatrix} = \beta^2 \begin{bmatrix} H_x \\ H_y \end{bmatrix}, \tag{1}$$

and

$$\begin{bmatrix} P_{xx} & P_{xy} \\ P_{yx} & P_{yy} \end{bmatrix} \begin{bmatrix} E_x \\ E_y \end{bmatrix} = \beta^2 \begin{bmatrix} E_x \\ E_y \end{bmatrix}, \tag{2}$$

where P_{ij} and Q_{ij} are coefficient matrix elements, E_x and E_y are electric field components, and H_x and H_y are magnetic field components respectively in the x direction and the y direction. If geometrical parameters, electromagnetic parameters and working wavelength are given, then propagation constant β, effective index n_{eff} and the distribution of magnetic field of each mode can be obtained by solving the eigenvalue equation (1). This eigenvalue problem is solved by Arnoldi arithmetic,[32] which can be used to deal with the matrix eigenvalue problem with a large complex coefficient matrix. Then substituting propagation constant β into Eq.(2), the electric distribution in the cross section of the corresponding mode can be obtained by solving these linear algebraic equations.

In the present paper, 601 × 601 lattices are adopted to discretize the whole computational domain, and their 20 layers are perfectly matched absorbing boundary layers that are used to truncate the lattices. The spatial discretization distance is $\Delta x = \Delta y = 1.0$ nm. The accuracy of the finite-difference frequency-domain (FDFD) code adopted in this paper has been validated in our previous work.[33]

Because the primary materials of which the SPWs are made are noble metals, there is a complex relation between the dielectric constant and the frequency of lightwave. In our calculation, the dielectric constants of the silver film at different wavelengths are $-88.9443 + 2.0557j$ ($\lambda = 1.30$ μm), $-125.7350 + 3.2330j$ ($\lambda = 1.55$ μm), and $-172.724 + 5.3154j$ ($\lambda = 1.80$ μm),[34] the dielectric constant of the background is 2.1025.

3. Results and discussion

Many modes are supported by the structure shown in Fig.1, and here we investigate mainly the symmetric mode.

Firstly, the distributions of the energy flux density S_{zr} of the symmetrical mode with different values of radius r at $\lambda = 1.55$ μm are calculated and shown in Fig.2. Here the energy flux density is defined as $S_{zr} = \text{Re}(E_x H_y - E_y H_x)$, and E_x, E_y, H_x and H_y are components of electric and magnetic fields in Eqs.(1) and (2) respectively. Figures 2(a) and 2(b) correspond to two conditions respectively.

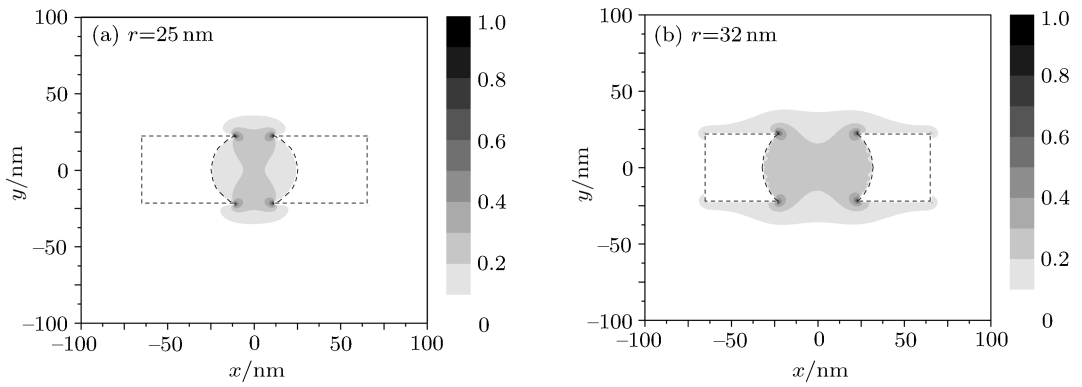


Fig.2. Distributions of energy flux density of the symmetrical mode supported by the structure shown in Fig.1 with $b = 65$ nm, $t = 22$ nm, $r = 25$ nm (a) and $r = 32$ nm (b) at $\lambda = 1.55$ μm, where dashed lines indicate the corresponding outlines of the structure.

Here we have selected the parameters of interest to us. These two figures show that the energy flux density is distributed mainly in the region of the arc slot. The closer it is to the sharp-angles of the four corners formed by two arcs, the stronger the energy flux density along the vertical direction will be. When the radius increases, the mode area increases correspondingly.

Secondly, we investigate the dispersion properties of the SPW shown in Fig.1. The dependences of effective index $\mathrm{Re}(n_{\mathrm{eff}})$ on radius are studied when $b = 55$, 65 and 75 nm, $t = 20$, 22 and 24 nm, and $\lambda = 1.55$ μm, and the results are shown in Fig.3. Here the effective index is defined as $\mathrm{Re}(n_{\mathrm{eff}}) = \mathrm{Re}(\beta\lambda/2\pi)$, where β is the complex propagation constant of SPP and λ is the free-space wavelength. From Fig.3, it can be seen that the effective index curves can be separated into three groups, corresponding to $b = 55$, 65 and 75 nm, respectively. When the value of b increases, the effective index decreases. In each group of curves, the larger the parameter t is, the steeper the curve will be. This indicates that the effective index is easily influenced by parameters b and t. The dependences of the effective index $\mathrm{Re}(n_{\mathrm{eff}})$ on radius are investigated when $b = 65$ nm, $t = 22$ nm, $\lambda = 1.80$, 1.55 and 1.30 μm, and the results are shown in Fig.4. The curves of the effective index have the same trends of variation with the arc radius at different working wavelengths, specifically, as the value of r increases, the effective index decreases. With the same radius, when the working wavelength becomes large, the effective index becomes smaller correspondingly.

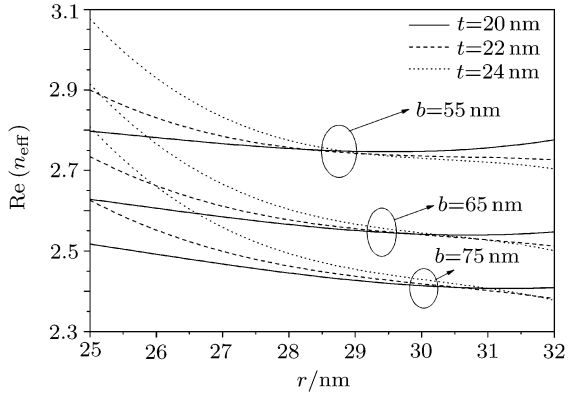


Fig.3. Dependences of the real part of the effective index on the structural parameters at $\lambda = 1.55$ μm.

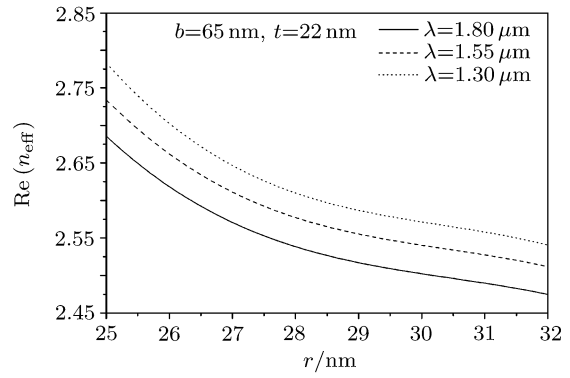


Fig.4. Dependences of the real parts of the effective index on slot radius at different wavelengths, $b = 65$ nm and $t = 22$ nm.

Thirdly, we investigate the dependence of the propagation length L_{prop} of the symmetric mode of the SPW shown in Fig.1 on radius. Here the propagation length is defined as $L_{\mathrm{prop}} = 1/\mathrm{Im}(\beta)$, where β is a complex propagation constant of the symmetric mode of the SPP. Results are shown in Fig.5, where $\lambda = 1.55$ μm, $b = 55$, 65 and 75 nm, $t = 20$, 22 and 24 nm. In Fig.5, it can be seen that the curves are separated into three groups, corresponding to $b = 55$, 65 and 75 nm separately. When the value of parameter b decreases, the propagation length increases. In each group of curves, the curve gradient is influenced by the value of parameter t. This indicates that the propagation length is easily influenced by parameters b and t. The relationships between propagation length and radius are investigated when $b = 65$ nm, $t = 22$ nm, $\lambda = 1.80$, 1.55 and 1.30 μm separately. As shown in Fig.6, the curves of the propagation length have the same trends of variation with the arc radius at different working wavelengths, or rather, as r increases, the propagation length increases. With the same radius, when the working wavelength becomes large, the propagation length becomes large correspondingly.

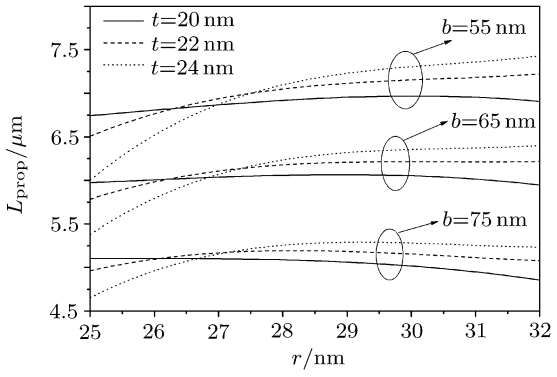


Fig.5. Dependences of the propagation length on the structural parameters at $\lambda = 1.55$ μm.

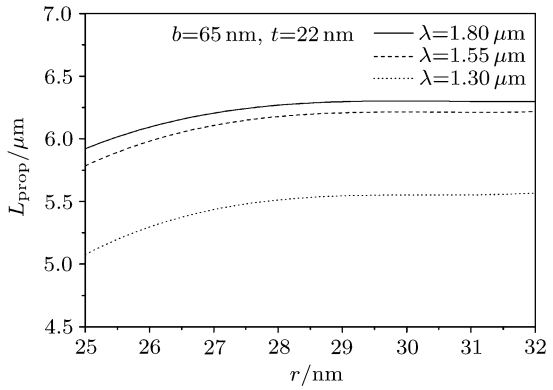


Fig.6. Dependences of the propagation length on slot radius at different working wavelengths, $b = 65$ nm and $t = 22$ nm.

Then, we investigate the dependence of the mode area of the symmetric mode supported by the SPW shown in Fig.1 on radius. Here, the mode area is defined as the distribution area of the energy flux density S_{zr} when its altitude descends from 100% to 10%. Results are shown in Fig.7, where $\lambda = 1.55$ μm, $b = 55$, 65 and 75 nm, $t = 20$, 22 and 24 nm. In order to see the results clearly, their curves are shown in three figures, separately, corresponding to $b = 55$, 65 and 75 nm. It can be seen that curves in each figure have similar trends. The mode area is about 2×10^{-3}–5×10^{-3} μm^2, which is beyond the diffraction limit. The mode area is insensitive to the value of parameter b. In each figure, the mode area increases with the increases of the value of parameter r, and the curve gradient is influenced by the value of parameter t. The relationships between mode area and radius are investigated when $b = 65$ nm, $t = 22$ nm, $\lambda = 1.80$, 1.55, and 1.30 μm separately. As shown in Fig.8, the curves of the mode area also have the same trends of variation with arc radius r at different working wavelengths, specifically, as r increases, the mode area increases. With the same value of radius r, as the working wavelength increases, the mode area becomes large.

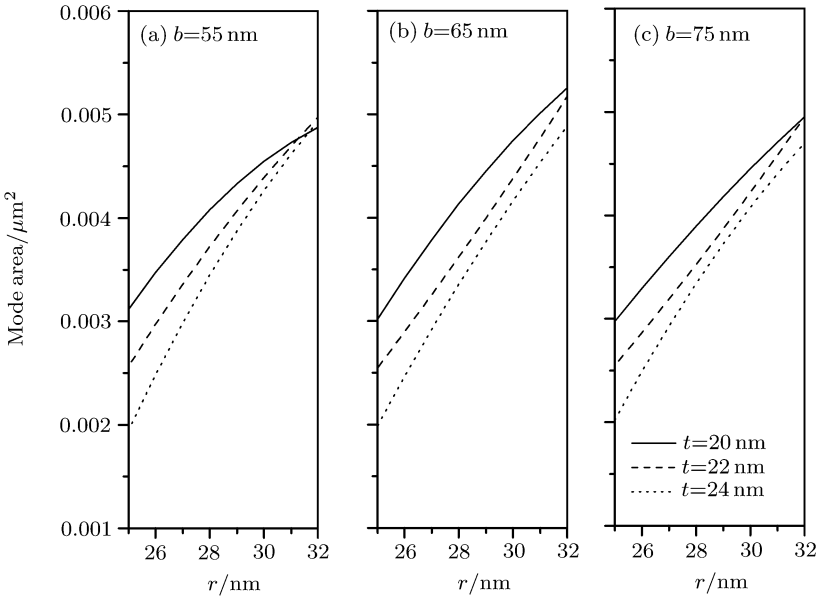


Fig.7. Dependences of the mode area on the structural parameters at $\lambda = 1.55 \mu m$.

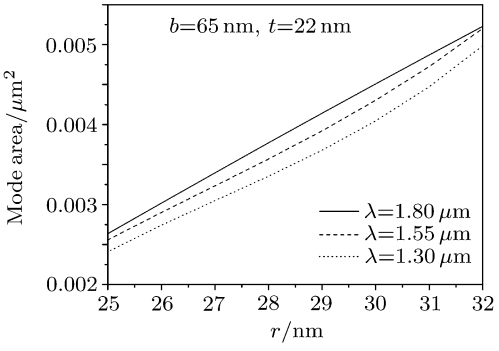


Fig.8. Dependences of the mode area on slot radius at different working wavelengths, $b = 65$ nm and $t = 22$ nm.

Finally, the propagation properties of the symmetric mode supported by the SPW with an arc slot shown in Fig.1 are compared with those in the case of the SPW with a straight slot[31] shown in Fig.9. Geometrical parameters of the SPW shown in Fig.9 are width $2b$, height $2t$, and slot width $2a$. Corresponding to Fig.2, the distribution of the energy flux density of the symmetric mode supported by the structure with different slot widths are shown in Fig.10. It can be seen from Fig.10 that although the distribution of the energy flux density becomes stronger in

the corners, most of energy flux is confined in the region between two straight sides. This phenomenon is different from that shown in Fig.2. Curves of effective index, propagation length and mode area of the symmetric modes supported by the two structures change with slot radius (or width), when $\lambda = 1.55$ μm, $b = 65$ nm, $t = 22$ nm and r or a=25–32 nm, are shown in Figs.11–13, respectively. From Figs.11–13, it can be seen that the curves of the effective index and propagation length of the symmetric mode supported by the SPW with straight slot are all below those in the case with arc slot in the computational region of slot radius (or width), but the curve of the mode area of the symmetric mode supported by the SPW with straight slot is above that in the case with arc slot in the computational region of slot radius (or width). This is because compared with the modes suppoted by the SPW with arc slot, the modes supported by the SPW with straight slot are tightly confined in the surface of the whole straight side, and there is strong interaction between SPP and metals, which consequentially leads to the drop of the effective index and the decrease of propagation length and mode area. These phenomenon indicate that the SPW with arc slot has better propagation properties than the SPW with straight slot.

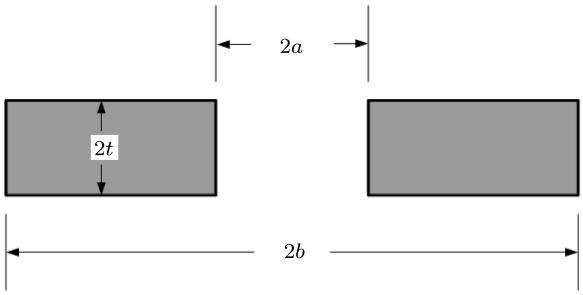


Fig.9. Cross section of the finite width plasmonic waveguide with a straight slot.[35]

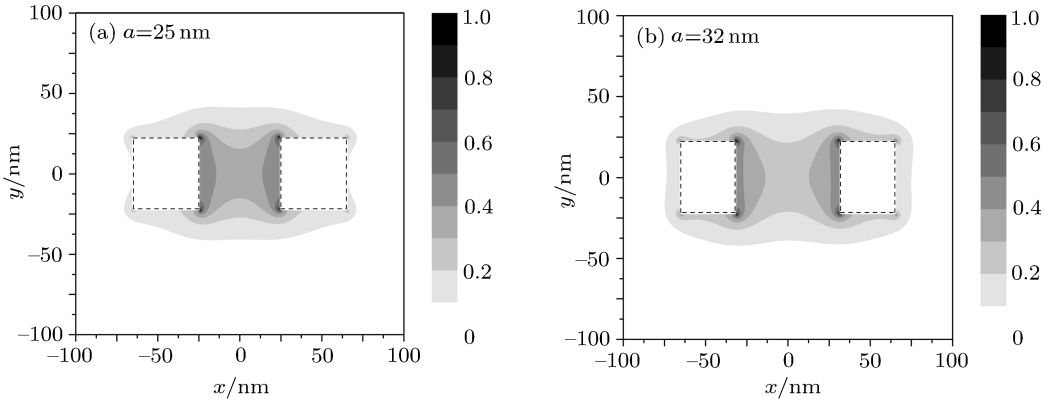


Fig.10. Distributions of the energy flux density of the symmetrical mode supported by the structure shown in Fig. 9 with $b = 65$ nm, $t = 22$ nm, $a = 25$ (a) and 32 nm (b) at $\lambda = 1.55$ μm, where dashed lines in (a) and (b) indicate corresponding outlines of the structure.

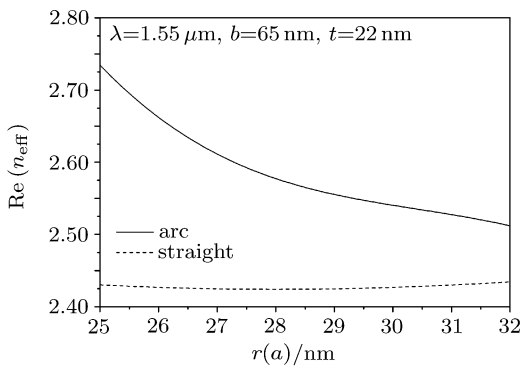


Fig.11. Dependences of the effective index on slot radius (or slot width) for different structures.

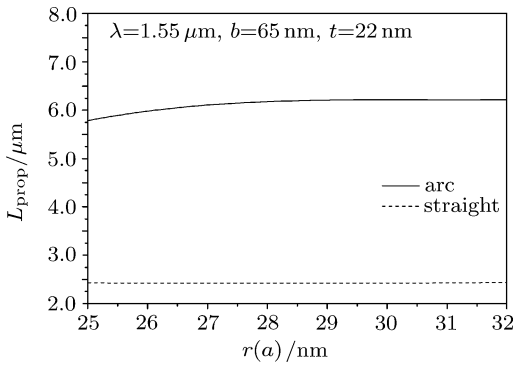


Fig.12. Dependences of propagation length on slot radius (or slot width) for different structures.

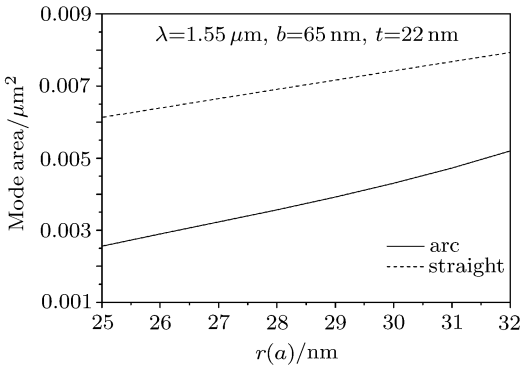


Fig.13. Dependences of the mode size on the slot radius (or slot width) for different structures.

4. Conclusion

We have investigated the propagation properties of the symmetric mode supported by a modified surface plasmonic waveguide with an arc slot. Results show that at a working wavelength of 1.55 μm, the energy flux density is mainly distributed in the four corners formed by two arcs, and the closer to the sharp-angle it is, the stronger the energy flux density will be. As the arc radius increases, the region of modal distribution increases. The effective index, the propagation length and the mode area of the symmetric mode are easily influenced by the width and the height of the waveguide. The trends of variation in each graph of the effective index, propagation length and mode area with arc radius are similar at different wavelengths. With the same radius, when the wavelength increases, the effective index decreases while the propagation length and mode area increase. By comparison, it is shown that the SPW with an arc slot has better propagation properties than the SPW with a straight slot. This work may be helpful for applying the slot SPW to integrated photonics.

References

[1] Barnes W L, Dereux A and Ebbesen T W 2003 *Nature* **424** 824
[2] Ozbay E 2006 *Science* **311** 189
[3] Bozhevolnyi S I, Volkov V S, Devaux E, Laluet J Y and Ebbesen T W 2006 *Nature* **440** 508
[4] Maier S A 2006 *IEEE J. Sel. Topics Quantum Electron.* **12** 1671
[5] Economou E N 1969 *Phys. Rev.* **182** 539
[6] Berini P 1999 *Opt. Lett.* **24** 1011
[7] Jung J, Sondergaard T and Bozhevolnyi S I 2007 *Phys. Rev.* B **76** 035434
[8] Guo J and Adato R 2008 *Opt. Express* **16** 1232
[9] Takahara J, Yamagishi S, Taki H, Morimoto A and Kobayashi T 1997 *Opt. Lett.* **22** 475
[10] Yang P F, Gu Y and Gong Q H 2008 *Chin. Phys.* B **17** 3880
[11] Tanaka K and Tanaka M 2003 *Appl. Phys. Lett.* **82** 1158
[12] Kusunoki F, Yotsuya T, Takahara J and Kobayashi T 2005 *Appl. Phys. Lett.* **86** 211101
[13] Gordon R and Brolo A G 2005 *Opt. Express* **13** 1933
[14] Pile D F P, Ogawa T, Gramotnev D K, Matsuzaki Y, Vernon K C, Yamaguchi K, Okamoto T, Haraguchi M and Fukui M 2005 *Appl. Phys. Lett.* **87** 261114
[15] Liu L, Han Z and He S 2005 *Opt. Express* **13** 6645
[16] Pile D F P, Ogawa T, Gramotnev D K, Okamoto T, Haraguchi M, Fukui M and Matsuo S 2005 *Appl. Phys. Lett.* **87** 061106
[17] Lu J Q and Maradudin A A 1990 *Phys. Rev.* B **42** 11159
[18] Chen S L , Shakya J and Lipson M 2006 *Opt. Lett.* **31** 2133
[19] Pile D F P and Gramotnev D K 2004 *Opt. Lett.* **29** 1069
[20] Lee I, Jung J, Park J, Kim H and Lee B 2007 *Opt. Express* **15** 16596
[21] Arbel D and Orenstein M 2008 *Opt. Express* **16** 3114
[22] Wang B and Wang G P 2004 *Appl. Phys. Lett.* **85** 3599
[23] Chen L, Wang B and Wang G P 2006 *Appl. Phys. Lett.* **89** 243120
[24] Wang G P, Wang B 2006 *J. Opt. Soc. Am.* B **23** 1660
[25] Wang B and Wang G P 2007 *Appl. Phys. Lett.* **90** 013114
[26] Quinten M, Leitner A, Krenn J R and Aussenegg F R 1998 *Opt. Lett.* **23** 1331
[27] Maier S A , Kik P G, Atwater H A, Meltzer S, Harel E, Koel B E and Requicha A G 2003 *Nature Materials* **2** 229
[28] Zhang H X, Gu Y and Gong Q H 2008 *Chin. Phys.* B **17** 2567
[29] Zhu Z and Brown T G 2002 *Opt. Expres* **10** 853
[30] Guo S P, Wu F, Albin S, Tai H and Rogowski R S 2004 *Opt. Expres* **12** 3341
[31] Yu C P, Chang H C 2004 *Opt. Express* **12** 6165
[32] Arnoldi W E 1951 *Quart. Appl. Math.* **9** 17
[33] Xue W R, Guo Y N, Li P and Zhang W M 2008 *Opt. Express* **16** 10710
[34] Johnson P B and Christy R W 1972 *Phys. Rev.* B **6** 4370
[35] Veronis G, Fan S 2007 *J. Lightwave Tech.* **25** 2511